

# Simulation of Bio-medical Waveguide in Mechanical and Optical Fields

Y. Xin<sup>1\*</sup>, A. Purniawan<sup>1</sup>, L. Pakula<sup>1</sup>, G. Pandraud<sup>2</sup>, P. J. French<sup>1</sup>

<sup>1</sup>Electronic Instrumentation Laboratory, TU Delft, the Netherlands

<sup>2</sup>Electronic Component, Technology and Materials, TU Delft, the Netherlands

\* Mekelweg 4, Delft, The Netherlands, x.yu@tudelft.nl

**Abstract:** This paper presents a freestanding waveguide to achieve the goal of detecting anastomosis leakage after colon surgery in early stage. The freestanding part is a thin membrane consisting of TiO<sub>2</sub> rib and SiN ridge. This freestanding waveguide is designed both mechanically and optically to maintain mechanical stability during fabrication and detection process, and at the same time guarantee the detection sensitivity. It utilises evanescent waves to detect the bacteria captured on both surfaces in freestanding area. Cladding factors and stress induced deformation are considered here to optimise the parameters. Through simulations, the final parameters are chosen to meet the medical requirements.

**Keywords:** Freestanding waveguide, evanescent wave, sensitivity, mechanical stability.

## 1. Introduction

An optical freestanding waveguide is designed to monitor patients after colon surgery. There is a possibility of leakage after surgery called anastomosis leakage which can lead to severe complications or even death. Detection time and detection sensitivity are dominant factors. Here, a freestanding waveguide is proposed to achieve this goal [1]. The freestanding part is a thin membrane consisting of TiO<sub>2</sub> rib and SiN ridge. TiO<sub>2</sub> is used for its high refractive index which is 2.45 [2], while that of SiN is 1.45. The contrast of refractive index makes it possible to confine light in the core part, which is TiO<sub>2</sub>. Furthermore, SiN has good mechanical properties. It serves to support the membrane and act as part of the waveguide simultaneously. Both surfaces are functionalised to be able to capture E-coli when patient's drain fluid is applied on it. There will be evanescent waves on the upper and lower surfaces of the freestanding part which can be used to sense the bacteria captured on the surfaces. The structural parameters are investigated here to meet the optimal design.

## 2. Structure Design and Simulation

The proposed bio-medical waveguide is composed of two channels, one for detection with freestanding part and another for reference without freestanding part. The freestanding part is shown in Figure 1. Both surfaces are functionalised with specific antibodies to catch E-coli in the drain fluid. Light is applied to the input port and guided by the waveguide. When light propagates through the freestanding region, there will be evanescent wave on both surfaces which will interact with the captured E-coli on it. The more E-coli there is in drain fluid, the more will be captured by antibodies on the surface and the greater the light absorption during the propagating process. By detecting the light loss during the transmission, the concentration of E-coli in the drain fluid can be measured. The cross section of the freestanding waveguide is shown in Figure 2. The structure needs to be well designed both optically and mechanically. The thickness of the freestanding membrane should be well defined. Mechanically, it should be thick enough to maintain mechanical stability during processing and operation. Optically, it should be thin enough to provide evanescent waves on both surfaces to detect the bacteria captured on both surfaces. The stress-induced deformation will also influence the light propagation in the waveguide, causing more scattering losses.

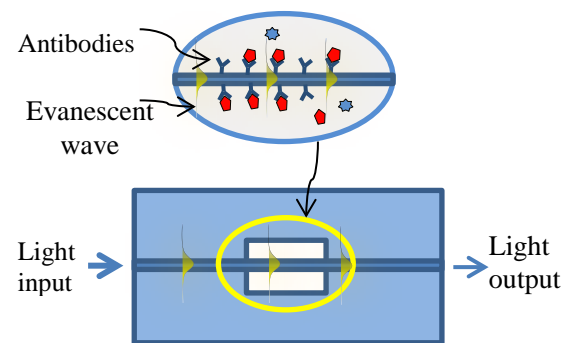


**Figure 1.** Schematic of the freestanding waveguide.

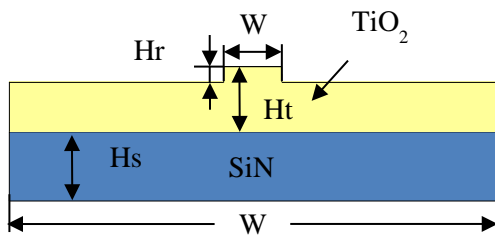


**Figure 2.** Cross section of the freestanding waveguide.

The evanescent wave profile is shown in Figure 3. Supposing that light propagates in one media with the refractive index of  $n_1$  and reached the interface with another media with the refractive index of  $n_2$  ( $n_1 > n_2$ ), when the incident angle is larger than the critical angle  $\theta_c$ , total internal reflection is achieved and most of the light is reflected. Only a small percentage of the reflected light penetrates through the interface, and propagates parallel to the surface in the plane of incidence creating an electromagnetic field in the medium adjacent to the interface [3]. The field is defined as the evanescent field. The evanescent wave intensity decays exponentially with the increasing distance from the interface. The equation is:

$$I(z) = I(0)e^{-z/d} \quad (1)$$

$I(z)$  is the intensity at the distance  $z$  from the interface,  $I(0)$  is the intensity at the interface.  $d$  is the penetration depth at  $\lambda$ , which is the wavelength of incident light in a vacuum.  $d$  is defined as:

$$d = \frac{\lambda}{4\pi \sqrt{n_1^2 \sin^2 \theta_i - n_2^2}} \quad (2)$$

Where  $\theta_i$  is incident light angle at the interface.

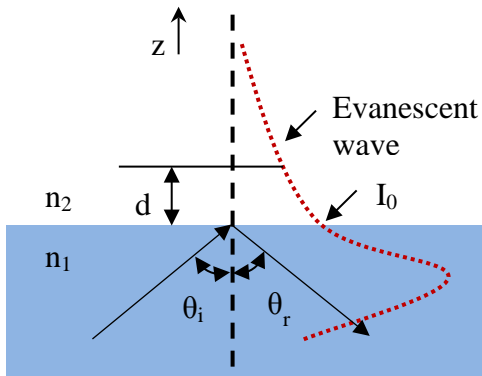


**Figure 3.** The evanescent wave profile.

### 3. Optical and Mechanical Simulation

According to the former design considering optical theory by former research work, the structure parameters are defined as  $Wt=3\mu\text{m}$ ,  $W=50\mu\text{m}$ ,  $Hr=50\text{nm}$ ,  $Ht=250\text{nm}$ ,  $Hs=250\text{nm}$ . The cross section is modelled in comsol to guarantee single mode confined in the core (shown in Figure 4).

From the equation (1) and (2),  $d$  is calculated to be greater than  $47.34\text{nm}$ . When  $\theta_i=90^\circ$ ,  $d$  is the minimum. When  $\theta_i=\theta_c$ ,  $d$  goes to infinity. The penetrate depth normally ranges between  $30\text{nm}$  and  $300\text{nm}$  [3]. Figure 5 shows the evanescent wave intensity along the  $z$  axis through the central of the cross section. As we can deduce from the simulation, the location where the evanescent wave intensity equals to  $I_0/e$  is at  $z=55.6\text{nm}$ , which fits in the theoretical calculation.

To compare the optical energy proportion outside the waveguide core in the air, here cladding filling factor is defined as the following:

$$\alpha = \frac{\iint_c \bar{E} dx dy}{\iint_\infty \bar{E} dx dy} \quad (3)$$

$E$  is the power flow density,  $c$  is the cladding area (air) of the waveguide.

For the current rib waveguide,  $Ht=250\text{nm}$ ,  $Hr=50\text{nm}$ ,  $Wt=3\mu\text{m}$ . The cladding filling factor is  $19.87\%$ . A sweep of  $Ht$  and  $Hr$  is set to get the optimal parameters.

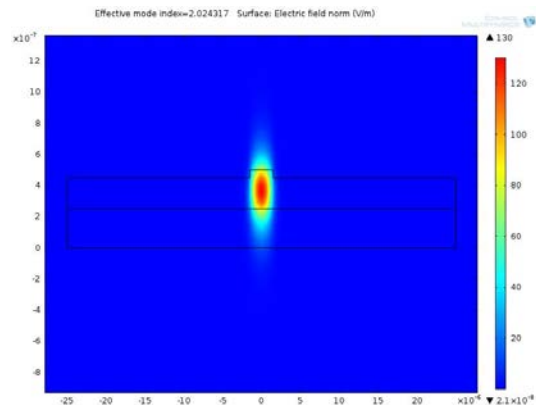


**Figure 4.** 2D simulation on the cross section of the waveguide

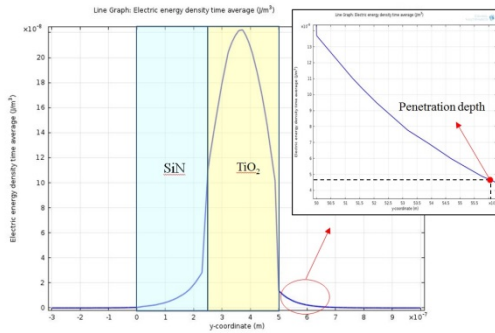


**Figure 5.** The evanescent wave intensity along the z axis through the central of the cross section.

For the freestanding waveguide, SiN cannot be too thin or thick, here 200nm and 250nm is set in the simulation considering the former experience. Wt stays the same which is 3 $\mu$ m, Hr changes from 10nm to 50nm with a step of 10nm, while Ht changes from 50nm to 250nm with a step of 50nm.

From the two figures below (Figure 6 and Figure 7), it can be concluded that when SiN is 200nm thick, Hr=10nm and Ht=50nm, the cladding filling factor reaches the maximum, which is 30.42%. The more evanescent light is in the cladding, the more sensitive the waveguide will be regardless of fabrication errors. When SiN is 250nm thick, Hr=20nm and Ht=50nm, the maximum cladding filling factor is 23.54%.

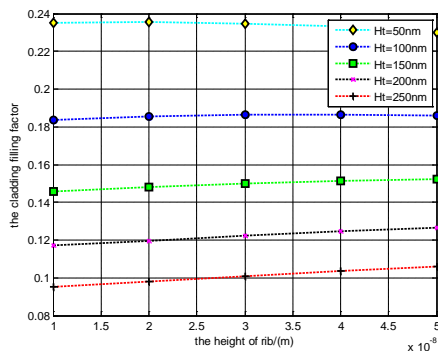


**Figure 6.** Cladding filling factor when SiN is 250nm.

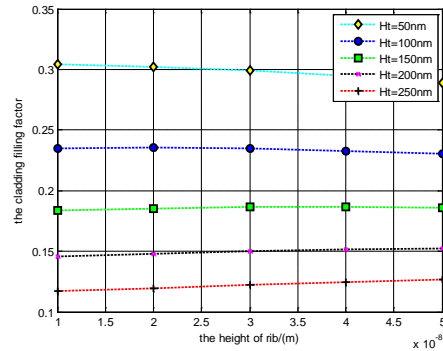


**Figure 7.** Cladding filling factor when SiN is 200nm.

To check how light propagates through the waveguides, 2D cross section develops into 3D model (Figure 8). Light is channelled by the waveguide in the core part. But in reality, inner stress will be induced during the fabrication process which may cause the freestanding bridge fracture or even break. Thus, solid mechanical physics is added to the model to check the mechanical stability. For TiO₂, inner stress is set as -120MPa [2], and for SiN, it is 125MPa [5]. As the simulation indicates (shown in Figure 9 and Figure 10), the maximum stress is 240MPa in SiN. The fracture strength of SiN is above 6GPa which is far more than the induced stress [4]. The structure is stable mechanically. And the maximum deformation of the rib where light is mainly confined is 0.21 $\mu$ m, it is quite a small deformation and its influence on light propagation can be neglected.

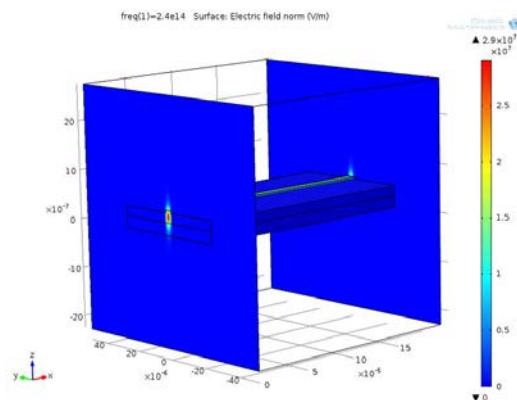


**Figure 8.** Light transmission in freestanding waveguide.

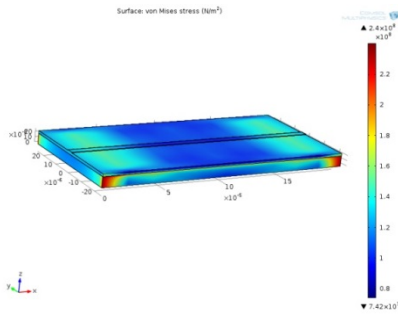


**Figure 9.** Stress induced by material inner stress.

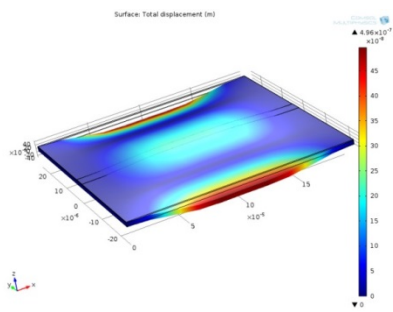


**Figure 10.** Deformation induced by material inner stress.

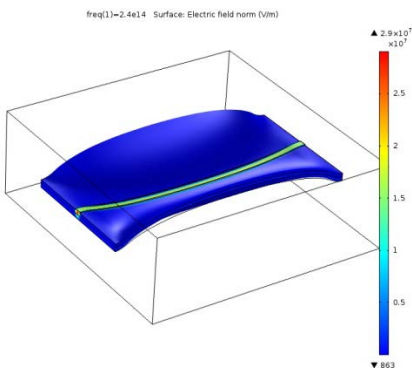


**Figure 11.** Combination of optical and mechanical simulation.

Finally, optical physics and mechanical physics are combined to see how light propagation is influenced by the deformation (shown in Figure 11). The power flow from the out port is integrated before and after deformation. Only 0.04% of energy is lost due to the small deformation.

#### 4. Conclusions

In this paper, the feasibility of freestanding waveguides for biomedical applications is demonstrated. Evanescent wave can be used for the purpose of detecting bacteria on the waveguide surface. Considering sensitivity and mechanical property, structural parameters are optimized. The final parameters are  $H_s=200\text{nm}$ ,  $H_r=10\text{nm}$ ,  $H_t=50\text{nm}$  and  $W_t=3\mu\text{m}$ .

#### 5. References

1. A. Purniawan, G. Pandraud, P. J French and P. M. Sarro,  $\text{TiO}_2$  Freestanding Thin Film as Evanescent Waveguide Sensor for Biomedical Application, *Transducers'11*, pp. 2506-2509 (2011).
2. A. Purniawan, P. French, G. Pandraud, and P. M. Sarro, An Investigation on ALD Thin Film Evanescent Waveguide Sensor for Biomedical Application, *Biomedical Engineering Systems and Technologies, CCIS, Vol. 127*, pp 189-196 (2011)
3. [Http://www.olympusmicro.com/primer/techniques/fluorescence/tirf/tirfintro.html](http://www.olympusmicro.com/primer/techniques/fluorescence/tirf/tirfintro.html)
4. W. Chuang , T. Luger, R.K. Fettig and R. Ghodssi, Mechanical Property Characterization of LPCVD Silicon Nitride Thin Films at Cryogenic Temperatures., *Journal of Microelectromechanical Systems, Vol. 13*, pp. 870-879 (2004)
5. P.J. French, P.M. Sarro, R. Mallee, E.J.M. Fakkeldij, R.F. Wolffenbuttel, Optimization of a low-stress silicon nitride process for surface-micromachining applications, *Sensors and Actuators A: physical, Vol.58*, pp. 149-157 (1997)

#### 6. Acknowledgements

The authors would like to acknowledge Comsol company for their support with comsol technical support, especially thanks for Ruud Börger and Durk de Vries.